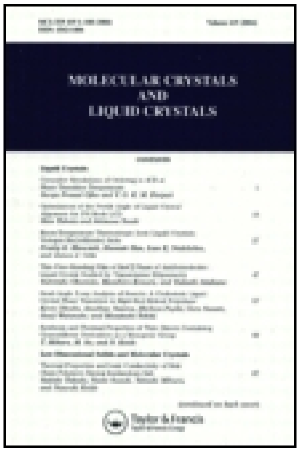

Molecular Crystals and Liquid Crystals Incorporating Nonlinear Optics
Publication details, including instructions for authors and subscription information:
http://www.tandfonline.com/loi/gmcl17

Exciton Annihilation Dynamics in Poly(Phenylenevinylene)

Mitsuhiro Furukawa [a] , Ken-Ichi Mizuno [a] , Atsuo Matsui [a] , Soonil D. D. V. Rughooputh [b] & William C. Walker [c]

[a] Depart. of Phys., Konan University, Okamoto, Kobe, 658

[b] Institute for Polymers and Organic Solids, University of California at Santa Barbara, Santa Barbara, California, 93106, USA

[c] Physics Department, University of California at Santa Barbara, Santa Barbara, California, 93106, USA

Version of record first published: 04 Oct 2006.

To cite this article: Mitsuhiro Furukawa , Ken-Ichi Mizuno , Atsuo Matsui , Soonil D. D. V. Rughooputh & William C. Walker (1990): Exciton Annihilation Dynamics in Poly(Phenylenevinylene), Molecular Crystals and Liquid Crystals Incorporating Nonlinear Optics, 183:1, 467-474

To link to this article: http://dx.doi.org/10.1080/15421409008047485

Mol. Cryst. Liq. Cryst., 1990, vol. 183, pp. 467–474
Reprints available directly from the publisher
Photocopying permitted by license only

Printed in the United States of America

EXCITON ANNIHILATION DYNAMICS IN POLY(PHENYLENEVINYLENE)

MITSUHIRO FURUKAWA, KEN-ICHI MIZUNO, ATSUO MATSUI,
SOONIL D. D. V. RUGHOOPUTH+ and WILLIAM C. WALKER++
Depart. of Phys. Konan University, Okamoto, Kobe 658
+Institute for Polymers and Organic Solids, University of California at Santa Barbara, Santa Barbara, California 93106, USA
++Physics Department, University of California at Santa Barbara, Santa Barbara, California 93106, USA

Abstract Luminescence processes of stretch-oriented poly(phenylenevinylene) (PPV) are investigated from a view point of exciton dynamics. It is found that PPV belongs to the category of strong exciton-phonon coupled system and provides a unique example where transient free-exciton luminescence is observable in time-integrated spectra at room temperature. It is also found that the height of the self-trapping barrier is 350 cm^{-1}, and the exciton tunneling rate is $(90\ \mathrm{ps})^{-1}$. The small luminescence quantum efficiency ($\sim$ 0.1 %) is explained as a result of a large lattice relaxation.

INTRODUCTION

Recent work on conjugated polymers has concentrated mostly on interrelations among quasi-particles, such as solitons, polarons, and bipolarons,[1-4] because production and transport of charge carriers are related to these quasi-particles. Friend and his coworkers [5,6] investigated optical properties of poly(phenylenevinylene) (PPV) from such a viewpoint, and analyzed the luminescence decay processes by monomolecular and bimolecular annihilation processes of excitons.

To reveal exciton relaxation process in detail, we have studied time-resolved luminescence spectra, luminescence decay times, the reflectance spectrum and pressure dependence of luminescence spectra, applying a weak optical excitation condition to avoid exciton-exciton interaction.

RESULTS AND dISCUSSION

Free and Self-Trapped Exciton Luminescence

Figures 1(a) and 1(b) show time-resolved luminescence spectra measured at 288 K. The specimen was excited by pulsed 303 nm light obtained from a dye laser. The figures on each curve show the time after excitation on a picosecond time scale. The time zero is taken to be the time where the light pulse has its maximum intensity. Each spectrum was integrated for a period of 9.8 ps. We shall use the notations (ex//-lumi//) and (ex⊥-lumi//) for excitation-luminescence combinations. The notation (ex//-lumi//) in the figure, for instance, indicates the exciting light and the luminescence are both polarized parallel to the stretched direction of a specimen. We will use the

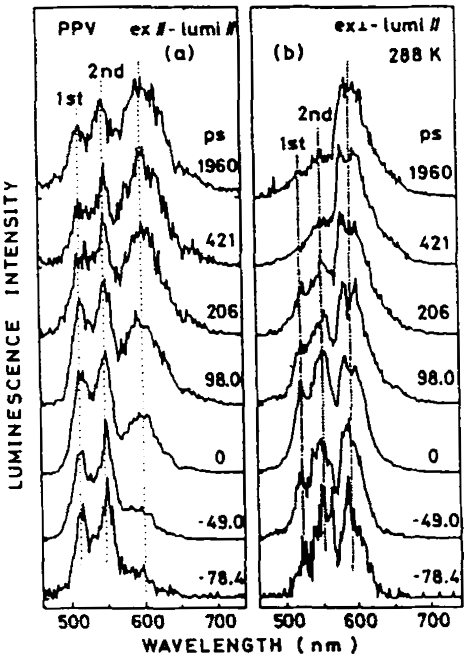

FIGURE 1. Time-resolved luminescence spectra measured at room temperature. Spectra are not corrected to the instrumental factors. The spectra are normalized at the maximum of each spectrum.

designation, first and second for the vibronic bands.

In the spectra two vibronic bands appear clearly at the early stage of the luminescence decay. With the lapse of time a broad band peaking at about 600 nm grew at the expense of vibronic bands. At reduced temperatures, this competitive behavior between the vibronic and broad bands is also found. Since the relative intensity of the broad band changed with time, the origin of the broad band differs from that of the vibronic bands. Luminescence spectra under pressure (Fig. 2) also show the presence of two luminescence origins. In Fig. 2, the pressure is indicated on each curve in GPa. The top diagram illustrates the spectrum at ambient pressure measured after a pressure cycle. Since this spectral shape is similar to the initial spectrum at 0.14 GPa, all the spectra we obtained under pressure are assumed to be reversible during a pressure cycle. Pressure dependence of the spectral shift and the pressure dependence of the intensity of vibronic bands both differ very much from those of the broad band. With increasing pressure, the vibronic bands are red shifted and their relative intensity decreases. On the other hand the broad band seems not to shift with pressure but its intensity increases.

Evidence of the presence of two luminescence components is substantiated by the presence of fast and slow components in luminescence decay.

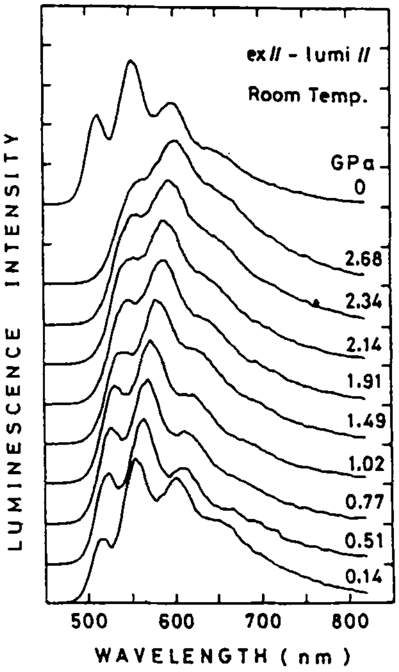

FIGURE2.Luminescence spectra (unpolarized)under pressure.

Fig. 3 shows (ex⊥-lumi//) luminescence decay curves monitored at short wavelengths and at long wavelengths. The wavelengths to monitor the decays were picked so that mutual contributions of vibronic and broad bands were separated as far as possible: The contribution of the broad band seems to be negligible in the shorter wavelength region while in the longer wavelength region the contribution of vibronic component is weak.

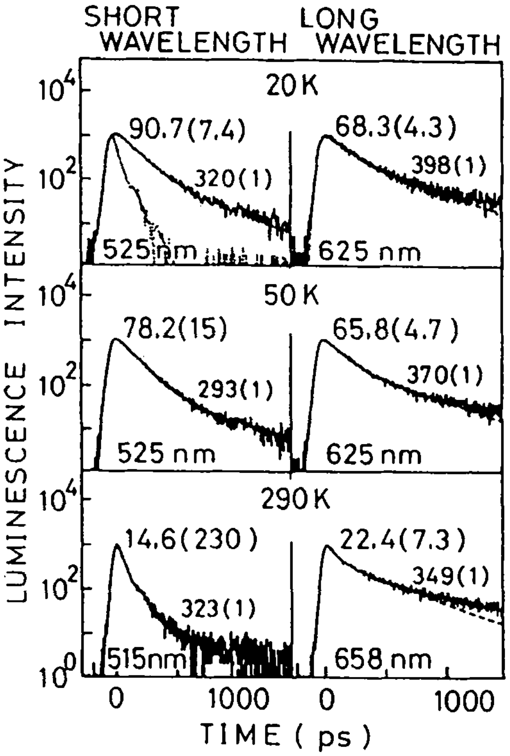

FIGURE 3. Luminescence decay curves monitored at short wavelengths (515 nm at 290 K, and 525 nm at 50 and 20 K) and at long wavelengths (658 nm at 290 K and 625 nm at 50 and 20 K). The wavelengths monitored are shown on each diagram. The ordinate gives the number of photons in a logarithmic scale.

A dotted curve on the left top diagram shows, as an example, time evolution of scattered exiting light from the specimen.

The decay curves were analyzed by a convolution technique, assuming luminescence decays with two exponential components. The decay times obtained, fast and slow, are shown on each curve on picoseconds. The figures in the parentheses show amplitudes of corresponding decays; the relative amplitude for slow components is taken to be unity. In decay curves at 290 K one finds that the relative amplitude of a fast component is large (amplitude = 230) at short wavelength (515 nm) but it is relatively small at long wavelength (658 nm) (amplitude = 7.3). The same relationship is established at 50 K (middle diagrams) and at 20 K (top diagrams). Since, as mentioned before, the vibronic bands dominate in the short wavelength region and the broad band dominates in the long wavelength region, observed facts give strong evidence that vibronic luminescence is responsible to the fast decay. On the other hand, the slow decay components at the long wavelengths can be attributed to the decay of the broad luminescence band. The slow decay components at short wavelength are attributed to broad background luminescence, while the fast decay components at long wavelengths are also attributed to the decay of vibronic bands.

In order to assign the origin of the vibronic bands we have measured reflectance spectrum at room temperature. We found a weak but clear bump at about 525 nm (2.36 eV). The position of this bump agrees well with the position of the first band in the time-resolved (ex⊥-lumi//) luminescence spectrum which is obtained immediately after pulse excitation. The bump is located 0.14 eV (1130 cm^{-1}) below the reported band-to-band transition energy (2.5 eV). This fact leads to a suggestion that the bump is caused by an optical transition from the ground state to the exciton state. The magnitude of the energy separation between the bump and the band-to-band transition, which is found to be 0.14 eV, is quite reasonable as an exciton binding energy. Therefore it is strongly suggested that vibronic luminescence originates from the free exciton state. Vibronic structures are probably attributed to intramolecular vibrations of polymer chains. The position of the maximum of the broad background luminescence band is located 3600 cm^{-1} longer wavelengths from the first vibronic band. Therefore, the broad band is attributed to relaxed excitons.

Potential Barrier and Transient Free-Exciton Luminescence

In time-resolved spectra at 288 K (Fig. 1(b)), the intensity of the broad band relative to vibronic bands increases with time, indicating that photoproduced excitons first relax to the free-exciton state and then to the relaxed states. This exciton relaxation process is well explained by an adiabatic potential energy curve which corresponds to a strong exciton-phonon coupled system. The adiabatic potential-energy diagram is schematically shown in Fig. 4.

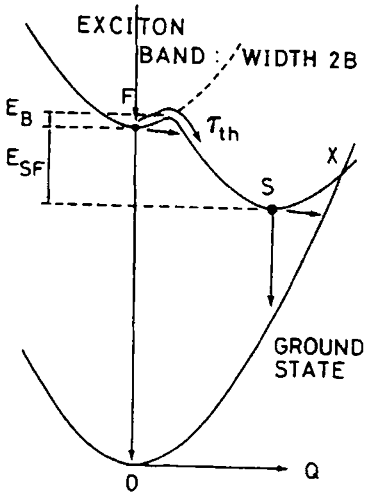

FIGURE 4. Schematic potential energy curve proposed for exciton states in PPV. The letters F and S denote the bottom of the free exciton band and the self-trapped state, respectively. The potential curve for the self-trapped state crosses that of the ground state at point X which is located in energy below the state F.

It has been well known [7] that when excitons interact strongly with phonons, a double-minimum adiabatic potential is established: The free-exciton state forms a quasi-stable state and the self-trapped state forms a stable state. When a double minimum potential is established, the annihilation probability τ^{-1} of transient free excitons is given as[8]

$$\tau^{-1} = \tau_o^{-1} + \tau_{th}^{-1} , \qquad (1)$$

where τ_{th}^{-1} is the non-radiative annihilation probability to the self-trapped state by surmounting the potential barrier and τ_o^{-1} is temperature-independent annihilation probability. τ_{th}^{-1} is temperature dependent and expressed as

$$\tau_{th}(T)^{-1} = \nu \exp(-E_B/kT) , \qquad (2)$$

where ν is the frequency factor, k the Boltzmann constant, T the temperature and E_B the height of the potential barrier. Similarly, one can express the intensity of free-exciton luminescence I (time-integrated) as

$$I(T)^{-1} = I(0\ K)^{-1} + A \times \exp(-E_B/kT), \qquad (3)$$

where A is a constant.

The values of τ^{-1} and $I(T)^{-1}$ are plotted in Fig. 5 as a function of temperature. Since the experimental data are well expressed by eqs. (1) and (3) for the decay time and for the luminescence intensity of the vibronic bands, respectively, the exciton relaxation model we suggested is probably valid for PPV. The barrier height 350 cm^{-1} obtained by eq. (3) corresponds to the potential barrier height E_B in Fig. 4. The inverse of the decay time at T=0 (90 ps $)^{-1}$ gives the exciton tunneling rate.

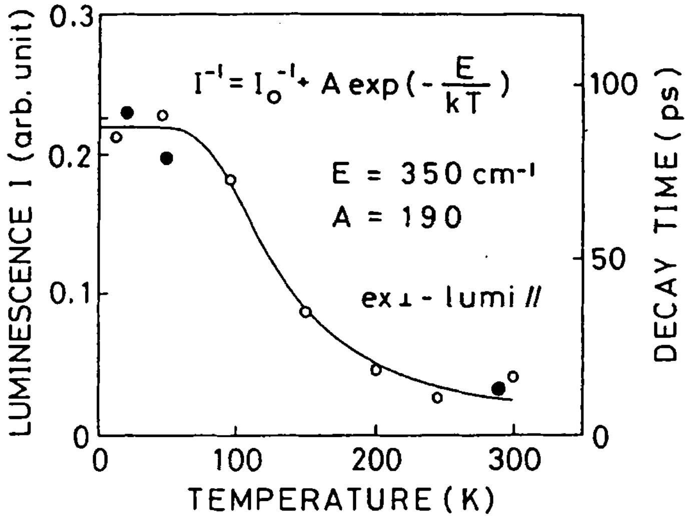

FIGURE 5. Integrated intensities of vibronic bands in time-integrated luminescence spectra, and decay times for the fast component in the short wavelength region in the (ex⊥-lumi//) combination. Open circles show the luminescence intensity I and solid circles decay times.

We emphasize here that, since $I(T)^{-1}$ observed is well expressed by eq. (3) in the temperature range 5 to 288 K, the free exciton luminescence we observed is attributed to transient free excitons (hot excitons). This is the first example that transient free-exciton luminescence appears in time-integrated luminescence at room temperature.

Non-Radiative Decay

If the relaxed state crosses the ground state at an energy only a little higher from the bottom of the self-trapped state (point X in Fig. 4), the non-radiative annihilation rate to the ground state would be considerable, which leads to a shorter decay time of relaxed excitons. In PPV, the decay time of relaxed excitons was of the order of a few hundred picoseconds and was almost independent of temperature, suggesting a non-radiative tunneling process through the barrier located at point X (ref. Fig. 4). Details of exciton annihilation processes are given elsewhere.[9]

REFERENCES

1. W. P. Su, J. R. Schrieffer and A. J. Heeger: Phys. Rev. Lett. **42** (1979) 1698.
2. S. Etemad, T. Mitani, M. Ozaki, T. C. Chung, A. J. Heeger and A. G. MacDiarmid: Solid State Commun. **40** (1981) 75.
3. C. V. Shank, R. Yen and R. L. Fork: Phys. Rev. Lett. **49** (1982) 1660.
4. J. Orenstein, S. Etemad and G. L. Baker: J. Phys. C. **17** (1984) L297.
5. K. S. Wong, D. D. C. Bradley, W. Hayes, W. Ryan, R. H. Friend, H. Lindenberger and S. Roth: J. Phys. C. **20** (1987) L187.
6. R. H. Friend, D. D. C. Bradley and P. D. Townsend: J. Phys. D (Appl. Phys.) **20** (1987) 1367.
7. Y. Toyozawa: Vacuum Ultraviolet Radiation Phsics (Pergamon-Vieweg, 1974) p317
8. H. Nishimura, C. Ohhigashi, Y. Tanaka and M.Tomura: J. Phys. Soc. Jpn. **43** (1977) 157.
9. M. Furukawa, K. Mizuno, A. Matsui, S. D. D. V. Rughooputh, J. Phys. Soc. Jpn. **58** (1989) 2976.